Cerebrotendinous xanthomatosis (van Bogaert-Scherer-Epstein disease): CT and MR findings.

M T Dotti, A Federico, E Signorini, N Caputo, C Venturi, G Filosomi and G C Guazzi

AJNR Am J Neuroradiol 1994, 15 (9) 1721-1726
http://www.ajnr.org/content/15/9/1721

Cerebrotendinous Xanthomatosis (van Bogaert-Scherer-Epstein Disease): CT and MR Findings

Maria Teresa Dotti, Antonio Federico, Enrico Signorini, Nevia Caputo, Carlo Venturi, Giuseppe Filosomi, and Gian Carlo Guazzi

PURPOSE: To describe the CT and MR findings in the brain and spinal cord of patients with cerebrotendinous xanthomatosis and to seek possible correlations between clinical, biochemical (cholestanol levels), and neuroimaging findings. **METHODS:** Ten patients with well-defined clinical and biochemical diagnoses of cerebrotendinous xanthomatosis were examined. Brain CT was performed in eight cases. In all patients MR was obtained using spin-echo and gradient-echo sequences. In eight patients spine MR was also performed. **RESULTS:** Neuroradiologic findings included diffuse cerebral and cerebellar atrophy. In half the cases, atrophy of the brain stem and corpus callosum was also found. In the majority of patients cerebellar bilateral focal lesions and mild white matter signal alterations were present. Spinal cord MR did not show signal abnormalities or atrophy. **CONCLUSIONS:** We found cranial alterations in patients with severe neurologic impairment, but there was no correlation with cholestanol plasma levels. No spinal cord abnormalities were present.

Index terms: Degenerative disease; Brain, computed tomography; Brain, magnetic resonance; Spinal cord, magnetic resonance

AJNR Am J Neuroradiol 15:1721–1726, Oct 1994

Cerebrotendinous xanthomatosis is a rare recessive inherited disorder of lipid metabolism, with a fairly constant clinical phenotype characterized by tendon xanthomas, early cataracts, mental deterioration, and spastic-ataxic signs (1). Neuropathologic studies have revealed granulomatous and xanthomatous lesions mainly in the cerebellum, the globus pallidus, and cerebellar peduncles. Only scattered collections of xanthoma cells have been reported in the white matter adjacent to the lateral ventricles. Demyelination and gliosis of the cerebellar and cerebral white matter and involvement of the spinal cord long tracts also have been observed (2–5). In 1965, van Bogaert described a case of a pure spinal form of cerebrotendinous xanthomatosis, without brain involvement (6).

The first computed tomography (CT) and magnetic resonance (MR) imaging studies revealed diffuse lesions in the cerebellar and cerebral white matter (7, 8). More recently, Fiorelli et al (9) in one case and Hokezu et al (10) in seven cases found focal cerebral and/or cerebellar lesions. Mild atrophy was also observed by the latter authors in all patients. MR of the spinal cord in cerebrotendinous xanthomatosis has been reported only once (11) and showed moderate cervical cord atrophy.

We describe the CT and MR findings in the brains and spinal cords of 10 patients with cerebrotendinous xanthomatosis and discuss them in light of prior literature.

Subjects and Methods

We examined 10 patients with cerebrotendinous xanthomatosis, followed during the last 6 years. The diagnosis was defined on the basis of clinical and biochemical parameters (cholestanol level greater than 1 mg/dL). The main clinical data and cholestanol levels are summarized

Received June 29, 1993; accepted after revision March 1, 1994.

This work was supported in part by a grant from CNR (to Dr Dotti).

From Istituto di Scienze Neurologiche (M.T.D., A.F., G.C.G.) and Istituto di Scienze Eidologiche e Radiologiche (C.V., G.F.), Università di Siena, and Divisione di Neuroradiologia, Ospedale di Perugia (E.S., N.C.), Perugia, Italy.

Address reprint requests to Maria Teresa Dotti, MD, Istituto di Scienze Neurologiche, viale Bracci, 53100 Siena, Italy.

AJNR 15:1721–1726, Oct 1994 0195-6108/94/1509–1721

Clinical data, cholestanol level, and brain MR findings

Case	1	2	3	4	5	6	7	8	9	10
Clinical data										
Sex	F	F	M	F	M	F	F	F	F	M
Age, y	36	38	35	40	35	44	51	41	36	49
Cataract	p	p	p	p	p	p	p	*	p	*
Xanthomas	p	p	p	p	p	p	p	p	p	p
Dementia	++	+	++	+	+	++	+++	−	−	++
Pyramidal signs	−	−	++	++	++	+	++	+	+	+++
Cerebellar signs	+	+	+	−	++	++	++	−	+	++
Seizures	p	−	p	−	−	p	−	−	−	−
Cholestanol[a]	3.0	2.9	2.3	2.8	3.2	1.7	np	3.5	4.2	1.7
MR findings										
Cerebral atrophy										
Cortical	+++	+	++	++	+++	++	+++	+	−	+++
Central	+++	−	++	+	++	++	+	−	−	+++
Cerebellar atrophy	+	+	++	+	++	+++	++	−	+	+++
Brain stem atrophy	++	−	−	−	+	+++	++	−	−	++
Corpus callosum atrophy	+	−	−	+	++	+	++	−	−	++
Focal lesions										
Cerebral	−	−	−	−	−	p	p	−	−	−
Cerebellar	p	p	X	−	X	X	X	−	−	X
Brain stem	p	−	−	−	−	p	p	−	−	−
Basal nuclei	−	−	−	p	−	p	p	−	−	p
White matter changes	−	+	−	+	+	+	++	+	−	++

Note.—p indicates present; *, opacity of crystalline lens; +, mild; ++, moderate; +++, severe; −, absent; np, not performed; and X, (presumed) xanthomas.

[a] Milligrams per deciliter (normal value, <1.0).

in the Table. Case 7, first observed elsewhere, was also included without performing cholestanol analysis in view of the specificity of the clinical picture. The clinical details of most of the cases already have been reported (12, 13). Four cases were familial (cases 1 and 2 and cases 3 and 4), the others sporadic. There was consanguineity in the families of cases 5, 8, and 9. Brain CT was performed in all but two cases (5 and 7). Axial sections of 10 mm with a 512 × 512 matrix were obtained; 5-mm sections were taken through the focal lesions. MR was performed using a 0.5-T system. For the brain, axial proton-density and T2-weighted sections 5 mm thick were obtained with 2-mm section gaps. Sagittal and coronal T1-weighted images were obtained without gaps. In all cases a spin-echo pulse sequence was used with parameters of 2000/28–100/2 (repetition time/echo time/excitations) for proton-density and T2-weighted axial images. A gradient-echo pulse sequence (Fourier-acquired steady-state technique) was used with parameters of 400/14/2 with a flip angle of 90° for coronal and sagittal T1-weighted images. For the spinal cords, T1-weighted images were obtained with parameters of 500/30/4. Gradient-echo T2-weighted contiguous images were obtained with parameters of 600/20/4, 5-mm thickness, and a flip angle of 18°. Additional gradient-echo axial T1-weighted images with variable gaps were also obtained with a flip angle of 90° and parameters of 400/14/4.

With the exception of cases 8 and 9, who were still untreated, MR was performed after chronic therapy with chenodiol (chenodeoxycholic acid).

Results

CT of the brain showed cerebral and/or cerebellar atrophy in all patients except in cases 8 and 9. Cerebellar bilateral hypodense lesions containing small calcificationlike opacities were found in cases 6 and 10 (Fig 1A). The brain MR findings are summarized in the Table. Cerebral cortical and central atrophy was observed in all but one patient and was severe in four. Cerebellar atrophy, absent only in case 8, ranged from mild to severe (Figs 2 and 3). Brain stem atrophy was observed in five patients. In the same patients, and in case 4, atrophy of the corpus callosum was also found (Fig 2). In some cases, high-signal focal lesions in T2-weighted images were detected in the cerebral (peritrigonal white matter and corona radiata in cases 6 and 7, respectively) and cerebellar (cases 1 and 2) white matter (Fig 3). Cerebellar nonhomogeneous areas of abnormal signal intensity were found in five patients (cases 3, 5, 6, 7, and 10) in the dentate nuclei bilaterally (Figs 1B–D). The hyperintense T2-weighted and hypointense T1-weighted images are probably caused by necrotic tissue (Figs 1B–D) as suggested by signal characteristics and neuropathologic observations in other cases of cerebrotendinous xantho-

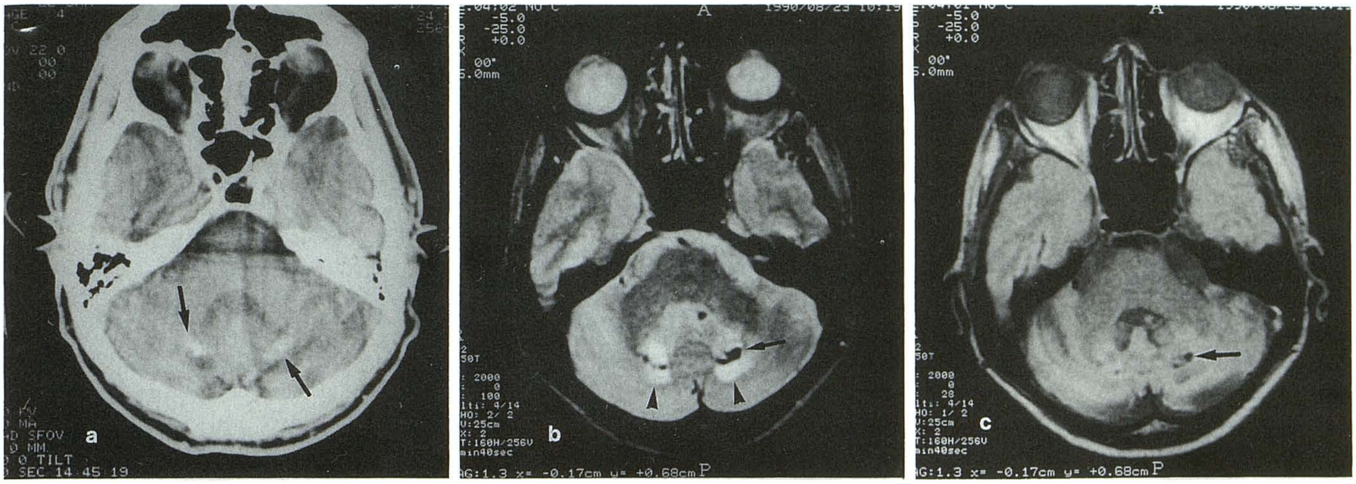

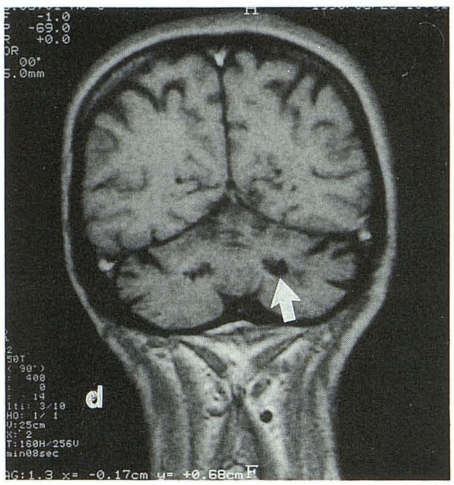

Fig 1. Case 10.

A, Axial CT showing bilateral focal hypodense lesions with small calcifications in the dentate nuclei (*arrows*).

B and *C*, Axial and *D*, coronal MR images through the posterior fossa consistent with bilateral cerebellar xanthomas. There are nonhomogeneous areas of abnormal signal intensity in the cerebellar hemispheres near the fourth ventricle. The strongly hyperintense areas on the T2-weighted images (*B, triangles*), moderately hyperintense on proton-density (*C*) and hypointense in T1-weighted images (*D*), suggest necrotic tissue. The markedly hypointense areas are calcium deposits (*arrows*).

matosis (2, 5) (Guazzi GC, unpublished data). The strongly hypointense areas in the three echoes suggest the presence of calcium deposits. Cerebellar lesions (xanthomas or otherwise) were always bilateral and almost symmetrical. High-signal lesions of the globus pallidus were evident in cases 6, 7, and 10 and of the thalamus in case 4 (Fig 4A). A small unilateral high-signal lesion was observed in the mesencephalon in cases 1 and 6 on T2-weighted images and in the pons in case 7. Mild, diffuse high-signal lesions (T2-weighted images) of periventricular white matter suggesting demyelination were evident in seven patients. MR of the spinal cords, performed in eight patients, did not reveal any abnormalities.

Discussion

Cerebrotendinous xanthomatosis is a rare but widespread metabolic disorder of lipid metabolism. We observed a considerable number of patients during a period of several years because our institute is one of the reference centers for neurogenetic disorders in Italy. The biochemical pathogenesis of cerebrotendinous xanthomatosis is related to abnormal bile acid synthesis caused by a defect in sterol 26-hydroxylase, a mitochondrial enzyme catalyzing the initial steps in the oxidation of the side chain of sterol intermediates in the metabolic pathway of cholesterol, resulting in increased plasma and tissue concentrations of cholestanol and decreased formation of cholic and chenodeoxycholic acid. Mutations in the sterol 26-hydroxylase gene in Jewish patients of Moroccan origin who had cerebrotendinous xanthomatosis recently have been reported (14). The tendons and central nervous system are primarily involved, but alterations also have been found in the peripheral nerves (12), muscle (15), and bone (16).

In the CT studies of Berginer et al (7) and Waterreus et al (8), high frequencies of diffuse hypodense lesions of the central white matter and mild atrophy are reported. More recently,

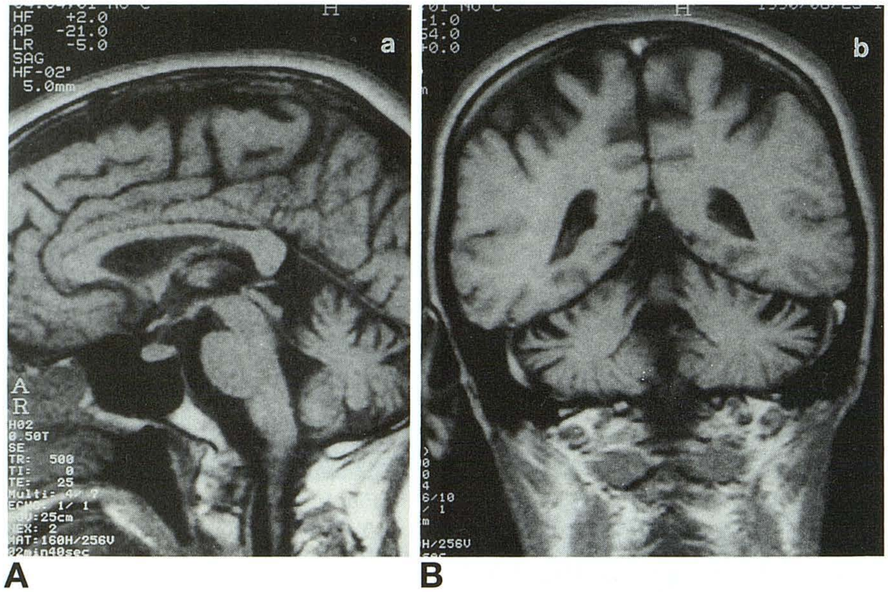

Fig 2. Case 7.
A, Sagittal and *B*, coronal images showing atrophy of the brain, brain stem, cerebellum, and corpus callosum.

Hokezu et al (10) performed brain MR in eight patients with cerebrotendinous xanthomatosis and found evidence of "multiple foci of high signal in various regions including the centrum semiovale, corona radiata, the white matter along the lateral ventricle, the globus pallidus and cerebellum" than of diffuse cerebral and/or cerebellar lesions. They did not draw definitive conclusions about the nature of the lesions observed by CT and MR. Moreover, they found only mild and sometimes equivocal cerebral and cerebellar atrophy, even in patients with very severe mental deterioration. In our study, all patients had cerebral and/or cerebellar atrophy, generally moderate or severe. Only cases 2, 8, and 9, without clear mental deterioration, showed insignificant cerebral and/or cerebellar atrophy. Atrophy of the brain stems and corpora callosa was present in five and six cases, respectively. Some authors (17, 18) recently focused on the high frequency of corpus callosum hypoplasia in childhood inherited metabolic diseases and suggested that this structure is particulary vulnerable to toxic metabolites. Because cerebrotendinous xanthomatosis is a late-onset neurometabolic disorder, high cholestanol levels could have a toxic effect on neurons and myelinated axons, leading to atrophy and secondary demyelination. We did not find significant diffuse lesions of the white matter apart from a slightly periventricular hyperintensity consistent with demyelination. In fact, necropsy studies have shown central demyelination (2, 5), and peripheral demyelination has

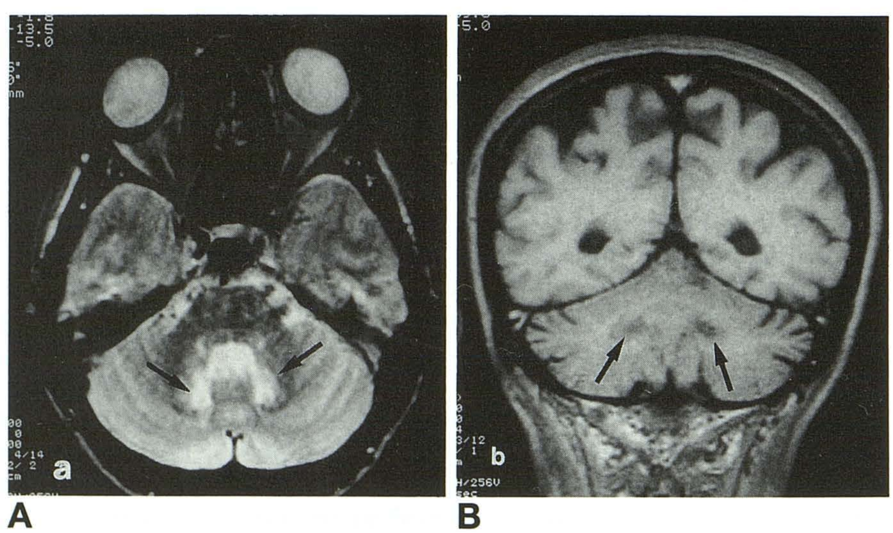

Fig 3. Case 1.
A, Axial and *B*, coronal images through the posterior cranial fossa. Focal areas of abnormal signal intensity (*arrows*) in the cerebellar dentate nuclei hyperintense on T2-weighted (*A*) and weakly hypointense on T1-weighted (*B*) images; cerebellar and cerebral atrophy.

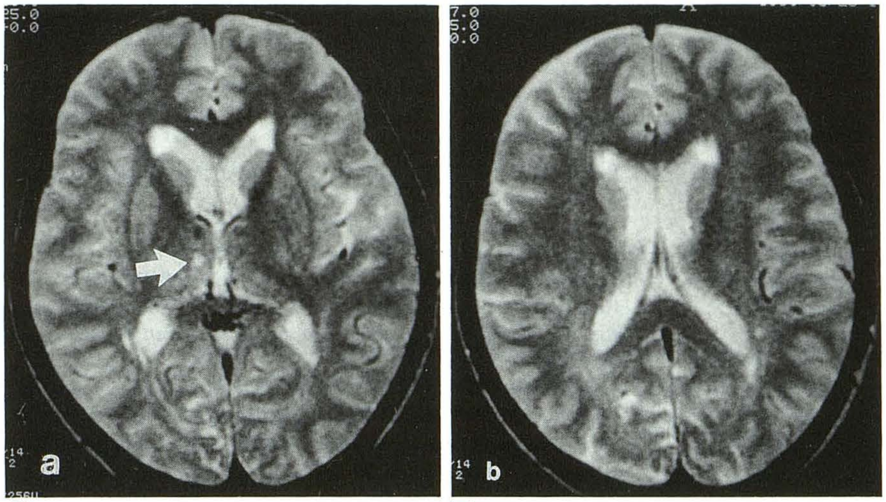

A B

Fig 4. Case 4. T2-weighted axial images showing mild periventricular hyperintensity. Note the presence of a high-signal abnormality in the right thalamus (*A, arrow*).

been described in neurophysiologic and nerve biopsy investigations of a large number of patients with cerebrotendinous xanthomatosis (12, 13, 19, 20). In a few cases, hyperintense focal lesions, probably reflecting demyelination or gliosis, were detected in the cerebral white matter, brain stem, and basal nuclei.

MR showed bilateral cerebellar lesions in seven patients, in five of them characterized by nonhomogeneous areas of abnormal signal intensity suggesting the presence of xanthomas formation. Cerebellar calcium deposits, confirmed in two cases by CT, are likely related to the necrosis associated with the xanthomas. As a whole, comparing clinical and neuroradiologic data, we found more brain neuroradiologic alterations (atrophy and focal lesions) in patients with severe neurologic impairment. On the other hand, in cases 8 and 9 with very mild clinical signs, no significant CT or MR alterations were evident. As in the cases of Hokezu et al (10), no correlations were present between cholestanol plasma levels and neuroradiologic abnormalities. However, at the time of radiologic examination, all our cases but two (cases 8 and 9) were taking chenodeoxycholic acid, a drug that has been demonstrated to reduce demyelinating lesions in the central (21) and peripheral nervous systems (13). MR combined with electrophysiological studies (electroencephalography and conduction velocities of peripheral nerve and evoked potentials) therefore could be other useful ways of evaluating the effect of therapy (13).

There is one previous report of spinal MR (11) performed in a case of cerebrotendinous xanthomatosis and revealing cerebral cord atrophy. We performed MR of spinal cords in eight patients. Despite neuropathologic reports of spinal long-tract involvement even in cases with the most common cerebral type of cerebrotendinous xanthomatosis (5, 6), and van Bogaert's description of a pure spinal form (6), in our cases MR failed to reveal any signal alterations or atrophy.

Acknowledgment

We thank Dr G. Salen for the determination of cholestanol levels.

References

1. Björkhem I, Skrede S. Familial diseases with storage of sterols other than cholesterol: cerebrotendinous xanthomatosis and phytosterolemia. In: Scriver CR, Beaudet AL, Sly WS, Valle D, eds. *The Metabolic Basis of Inherited Disease.* New York: Mc Graw-Hill, 1989:1283–1302
2. van Bogaert L, Scherer HJ, Epstein E. *Una Forme Cérébrale de la Cholestérinose généralisée.* Paris: Masson et Cie, 1937
3. van Bogaert L. Le cadre des Xanthomatoses et leurs differents types: Xanthomatoses secondaires. *Rev Med* 1962;17:433–443
4. Guillain G, Bertrand I, Godet-Guillain M. Etude anatomoclinique d'un cas de cholestérinose cérébrale. *Rev Neurol* 1942;74:249–263
5. Schimschock JR, Alvord EC, Swanson PD. Cerebrotendinous xanthomatosis: clinical and pathological studies. *Arch Neurol* 1968;18:688–698
6. van Bogaert L. Spinal cholesterolosis. *Brain* 1965;88:687–696
7. Berginer VM, Berginer DJ, Salen G, Shefer S, Zimmermann DR. Computed tomography in cerebrotendinous xanthomatosis. *Neurology* 1981;31:1463–1465

8. Waterreus RJ, Koopman BJ, Wolthers BG, Oosterhuis HJGH. Cerebrotendinous xanthomatosis (CTX): a clinical survey of the patient population in the Netherlands. *Clin Neurol Neurosurg* 1987;89:169–175
9. Fiorelli M, Di Piero V, Bastianello S, Bozzao L, Federico A. Cerebrotendinous xanthomatosis: clinical and MRI study (a case report). *J Neurol Neurosurg Psychiatry* 1990;53:76–78
10. Hokezu Y, Kuriyama M, Kubota R, Nakagawa M, Fujiyama J, Osame M. Cerebrotendinous xanthomatosis: cranial CT and MRI studies in eight patients. *Neuroradiology* 1992;34:308–312
11. Bencze KS, Vande Polter DR, Prockop LD. Magnetic resonance imaging of the brain and spinal cord in cerebrotendinous xanthomatosis. *J Neurol Neurosurg Psychiatry* 1990;53:166–167
12. Dotti MT, Salen G, Federico A. Cerebrotendinous xanthomatosis as a multisystem disease mimicking premature aging. *Dev Neurosci* 1991;13:371–376
13. Mondelli M, Rossi A, Scarpini C, Dotti MT, Federico A. Evoked potentials in cerebrotendinous xanthomatosis and effect induced by chenodeoxycholic acid. *Arch Neurol* 1992;49:469–475
14. Leitersdorf E, Reshef A, Meiner V, et al. Frameshift and splice-junction mutations in the sterol 27-hydroxylase gene cause cerebrotendinous xanthomatosis in Jews of Moroccan origin. *J Clin Invest* 1993;91:2488–2496
15. Federico A, Dotti MT, Volpi N. Muscle mitochondrial changes in cerebrotendinous xanthomatosis (letter). *Ann Neurol* 1991;30: 734–735
16. Federico A, Dotti MT, Loré F, Nuti R. Cerebrotendinous xanthomatosis: pathophysiological study on bone metabolism. *J Neurol Sci* 1993;115:67–70
17. Bamforth F, Bamforth S, Poskitt K, Applegarth D, Hall J. Abnormalities of corpus callosum in patients with inherited metabolic disease (letter). *Lancet* 1988;20:451
18. Kolodny EH. Agenesis of the corpus callosum: a marker for inherited metabolic disease? *Neurology* 1989;39:847–848
19. Katz DA, Scheinberg L, Horoupian DS, Salen G. Peripheral neuropathy in cerebrotendinous xanthomatosis. *Arch Neurol* 1985; 42:1008–1010
20. Voiculescu V, Alexianu M, Popescu-Tismana G, Pastia M, Petrovici A, Dan A. Polyneuropathy with lipid deposits in Schwann cells and axonal degeneration in cerebrotendinous xanthomatosis. *J Neurol Sci* 1987;82:89–99
21. Berginer WM, Salen G, Shefer S. Long term treatment of cerebrotendinous xanthomatosis. *N Engl J Med* 1984;311:1649–1652